Virchows Arch A (1987) 410:265–279

Virchows Archiv A

The application of various electron microscopic techniques for ultrastructural characterization of the human papillary heart muscle cell in biopsy material

Helge Dalen [1], Svein Ødegården [2], and Thorvald Sætersdal [2]

[1] Laboratory of Clinical Electron Microscopy and
[2] Cellular Cardiology Research Group, Institute of Anatomy, University of Bergen, Norway

Summary. Various electron microscopical techniques have been applied to biopsy material obtained from patients suffering from mitral stenosis in order to characterize the subcellular organization of the hypertrophied papillary muscle. Small pieces of the same sample were processed for correlative transmission – (TEM) and scanning – (SEM) electron microscopical studies. TEM was carried out on conventionally fixed tissue with or without *en bloc* staining with a Cu-Pb citrate solution, and on freeze fracture replicas, while cryofractured material was studied by SEM. Stereo electron micrographs of the Cu-Pb impregnated tissue and of the cryofractured material were especially useful for studying the spatial distribution and relationship between various cell organelles.

The myofilaments of the hypertrophied cells were arranged in a normal hexagonal pattern. Regions with irregular orientation of the myofibrils were occasionally seen. Accumulations of interfilamentous glycogen particles adjacent to the Z-bands were characteristic patterns of the contracted muscle cells. The extensive nexuses frequently observed in the subsarcolemmal regions may reflect functional alterations of the intercommunication between hypertrophied cells. The T-tubules were relatively few and irregularly distributed, and the complexity of the sarcotubular system (SR) revealed regional variations. Excellent visualization of the interior couplings between the SR and the T-tubules was achieved by studying thick sections of Cu-Pb impregnated tissue in the TEM.

The dense staining of the various intracellular membranes when compared with the almost unstained external membranes including the free cell surface, intercalated disc and T-system, strongly indicates differences in chemical and functional properties of the two membrane systems. *En bloc* staining resulted also in contrasted glycogen as well as components of the nucleolus and the heterochromatin. The biochemical basis for the selective staining remains obscure; it may be a result of binding of heavy metal ions to carboxyl groups of specific proteins, and/or it may represent deposits of lead phosphate.

Key words: Human heart – Hypertrophied papillary muscle – Intracellular membranes – Specific staining – Cryofracturing

Offprint requests to: H. Dalen, Laboratory of Clinical Electron Microscopy, University of Bergen, 5016 Haukeland Hospital, Norway

Introduction

The prevalent description in the literature of both the normal and pathological ultrastructure of human myocardium has been based almost exclusively on electron microscopical examinations of conventionally prepared thin sections of biopsy material (Sætersdal et al. 1976; Jones and Ferrans 1979; Ferrans and Butany 1983; Ferrans and Thiedemann 1983).

However, additional ultrastructural information can be obtained if the same biopsy material is subjected to other ultrastructural procedures. The advantages of a more extensive investigation are illustrated using the papillary muscle from pa-

tients with mitral stenosis as a model system. Although the amount of tissue available for morphological studies in such cases is very limited, it has been possible to process portions of the same sample using various electron microscopical techniques. These techniques include:

1) Transmission electron microscopy (TEM) of standard thin sections and of thin and thick sections of Cu-Pb impregnated material (Thiéry and Bergeron 1976), 2) TEM of freeze fracture replicas; and 3) scanning electron microscopy (SEM) of cryofractured material (Dalen et al. 1978). Stereo micrographs were also prepared from the cryofractured material and from the thick sections.

In the present communication our interest has been focused on the ultrastructural organization of the contractile material, the intercalated disc, the transverse-axial tubular system (T-system) and on the sarcoplasmic reticulum (SR) together with specific staining features of various intracellular structures. Ultrastructural information concerning other cellular components including the extracellular connective tissue, will be published elsewhere (Dalen 1987; Dalen et al. 1987).

Materials and methods

Biopsy material of mechanically overloaded ventricular papillary muscle was obtained during open heart surgery of two adult patients suffering from mitral stenosis. Immediately after surgical removal the tissue was immersed in ice-cold Hank's balanced salt solution and cut into small pieces before fixation in glutaraldehyde. The material was divided into four groups, and each group was processed according to one of the various methods described below.

Preparation for conventional TEM. The fixation was carried out overnight at 4° C in 2% glutaraldehyde followed by 1 h in ice-cold 1% OsO_4. Both fixatives were made up in 0.1 M cacodylate buffer (pH 7.2) with 0.1 M sucrose, vehicle osmolality = 300 milliosmols (Ericsson et al. 1978). The specimens were dehydrated in increasing concentrations of ethanol, passed through propylene oxide, and embedded in Epon 812 (Luft 1961). After polymerization thick (1 μm) and thin sections were prepared with a Reichert ultramicrotome. The thick sections were stained with toluidine blue (Trump et al. 1961) for examination in the light microscope, while the thin sections were contrasted with uranyl acetate (Watson 1958) and lead citrate (Reynolds 1963) and studied in a Philips 300 transmission electron microscope operated at 60 kV.

Preparation of thick sections for TEM. After fixation in glutaraldehyde as above the myocardial tissue was rinsed in distilled water and *en bloc* stained for 24 h at 4° C with a double copper and lead citrate solution (Cu-Pb impregnation) prepared according to the method described by Thiéry and Bergeron (1976). Subsequently, the specimens were rinsed thoroughly in distilled water and postfixed for an additional 24 h in 1% cacodylate-buffered OsO_4 at 4° C. Dehydration, embedding, polymerization and sectioning followed conventional procedures. Both thin and thick (1 μm) sections were picked up on naked copper grids (300 mesh). The thin sections with or without conventional contrasting were studied in the TEM at 60 kV, while the thick sections were examined without counterstaining at 80 or 100 kV. Stereo electron micrographs of the thick sections were obtained by tilting the goniometer stage plus and minus 6° from the zero position between two successive exposures.

Preparation for SEM. Tissue designated for SEM studies was fixed in glutaraldehyde as above, dehydrated, embedded in paraffin and cryofractured according to the technique described by Dalen et al. (1978). After removal of the embedding material with xylol, the fractured material was critical point dried from CO_2 using acetone as a transitional solvent, mounted on specimen holders and coated with gold according to the diode-sputter technique (Echlin 1975). The fractured surfaces were viewed in a Philips SEM 500 operated at 25 kV. Stereoscopic pictures were taken by tilting the goniometer stage 10° between two successive exposures.

Preparation of freeze fracture replica. Fixation of the myocardial tissue was carried out for 30 min at 4° C in 2% glutaraldehyde made up in isotonic cacodylate buffer as described above. Following 30 min of impregnation with 30% glycerol made up in the same buffer, the specimens were mounted on gold holders and quenched in melting Freon 22. The fracturing was conducted in a Balzer's freeze fracture apparatus and replicated with platinum-carbon. Following these treatments, the replicas were cleaned with a sodium hypochlorite solution, rinsed in distilled water, mounted on formvar coated grids and viewed in the TEM at 80 kV.

Results

With few exceptions the substructure of the contractile material appeared normal with transverse myofibrillar bands arranged in a regular alternating array (Fig. 1). However, since the biopsy material was fixed without mechanical stretching, the muscle fibers were preserved in a highly contracted state. Under such conditions the I-bands were absent, and the intrafibrillar glycogen particles of these bands had accumulated adjacent to the Z-bands (Fig. 2). Transverse sections through the A-band region revealed that the thin (actin) and thick (myosin) myofilaments were arranged in the characteristic hexagonal pattern (Fig. 3). The variable length of the actin myofilaments, in accordance with observations by Robinson and Winegrad (1977, 1979) in rat and frog myocardium, was manifested by the appearance of a few such structures in the M-band region.

The contractile material was generally arranged in parallel and discrete myofibrils separated by numerous mitochondria (Figs. 2, 4). In some regions, however, the contractile elements displayed a branching pattern (Fig. 5). In the contracted muscle the Z-bands appeared as prominent cross-ridges with occasionally superimposed T-tubules (Fig. 5). The deeply interlocking membranes of the intercalated disc contained a conglomerate of intermedi-

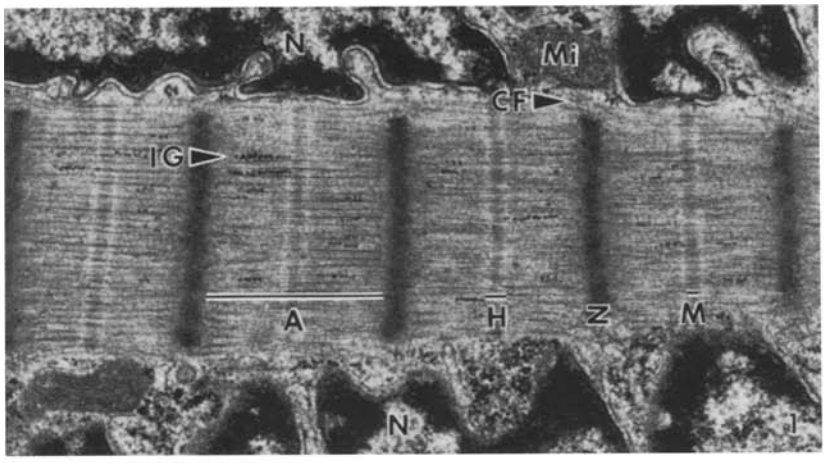

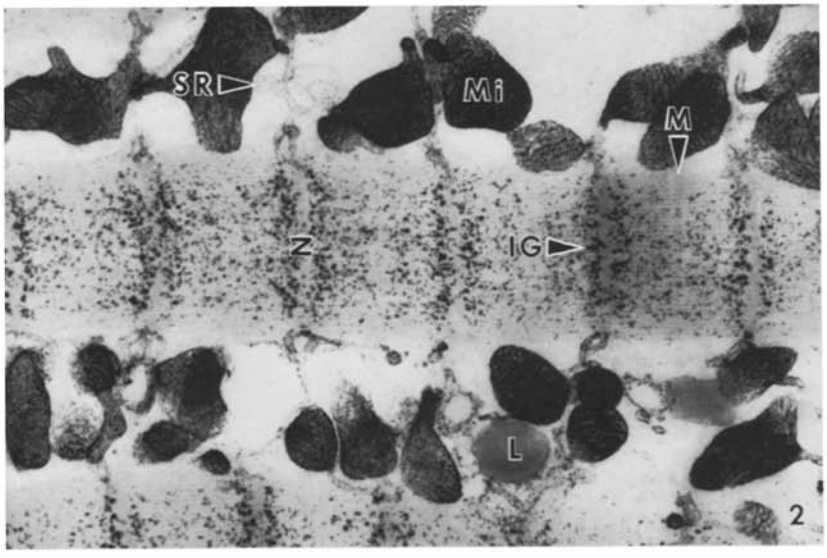

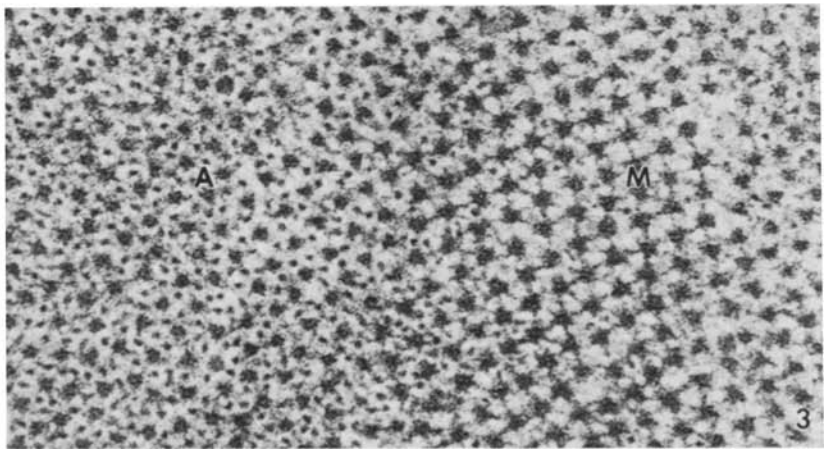

Fig. 1. Longitudinal section of a contracted myofibril running through a deep fold of the nuclear membrane. Most bands of the sarcomere (*Z, A, H, M*) are easily identified; I-band is absent. The rows of interfilamentous glycogen particles (*IG*) are excluded from the Z- and M-bands. Note the cytoskeletal filaments (*CF*) extending from the Z-band to the mitochondrial surface. *N*, nucleus ×25,000

Fig. 2. The accumulation of interfilamentous glycogen particles (*IG*) on each side of the Z-bands (*Z*) in the contracted muscle fiber is demonstrated in this 1 μm thick section from Cu-Pb impregnated tissue. *M*, M-band; *SR*, sarcoplasmic reticulum, *L*, lipid droplet; *Mi*, mitochondrion. ×18,000

Fig. 3. Transverse section through the A- and M-bands of a contracted myofibril. In the A-band (*A*) the myosin (thick) and actin (thin) filaments are arranged in a hexagonal pattern, while the M-band (*M*) is composed of an array of myosin filaments held in register by cross bridges. Note that a few actin filaments extend into this region. ×125,000

ate junctions, desmosomes and nexuses (gap junctions), of which the intermediate junctions constituted the major component (Fig. 6). A dense filamentous mat in which the actin filaments were anchored was located on the sarcoplasmic face of the intermediate junction. The desmosomes were smaller than the intermediate junctions, and their interspaces were filled with an electron-dense material. The nexuses, which in thin sections appeared as short segments of closely opposed cell membranes, were situated almost exclusively on the longitudinal faces of the intercalated disc. In the re-

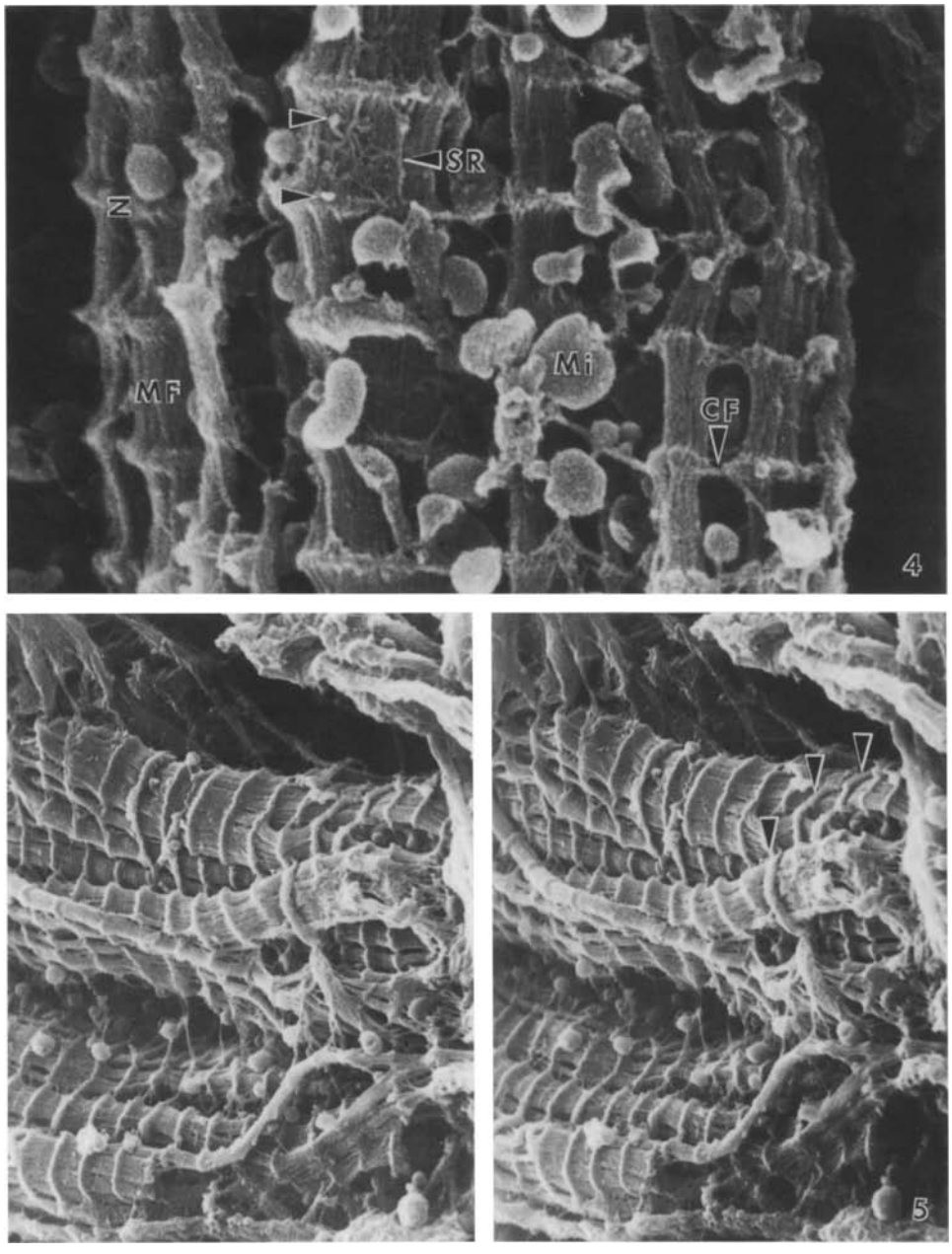

Fig. 4. A scanning electron micrograph of the myocardial cell interior. The myofibrils (*MF*) which are characterized by elevated Z-bands (*Z*), are surrounded by numerous mitochondria (*Mi*) of various shapes and sizes. A network of sarcoplasmic reticulum (*SR*) is closely applied to the myofibrillar surface. Bundles of cytoskeletal filaments (*CF*) interconnect the Z-bands of adjacent myofibrils. Structures interpreted as corbular SR are indicated by arrowheads, × 15,000

Fig. 5. Stereo-pair (10° tilt) of scanning electron micrographs demonstrating the branching pattern of the myofibrils. Transverse tubules superimposed on the elevated Z-bands are indicated by arrowheads. × 4,500

gion adjacent to the external cell surface, however, they were frequently seen as extensive and convoluted structures (Fig. 7). In thin sections of both conventionally fixed and stained tissue, as well as in Cu-Pb-impregnated material counterstained with uranyl acetate and lead citrate, the closely opposed membranes of the nexus appeared as a central dotted line (Fig. 8). A periodic electron-dense material was located on the sarcoplasmic side of the nexus. When cut at certain angles the nexuses revealed a periodic pattern of electron-dense strands traversing the electron-lucent space. The lattice of globular subunits (connexons) of the nexus' membranes were revealed in freeze-frac-

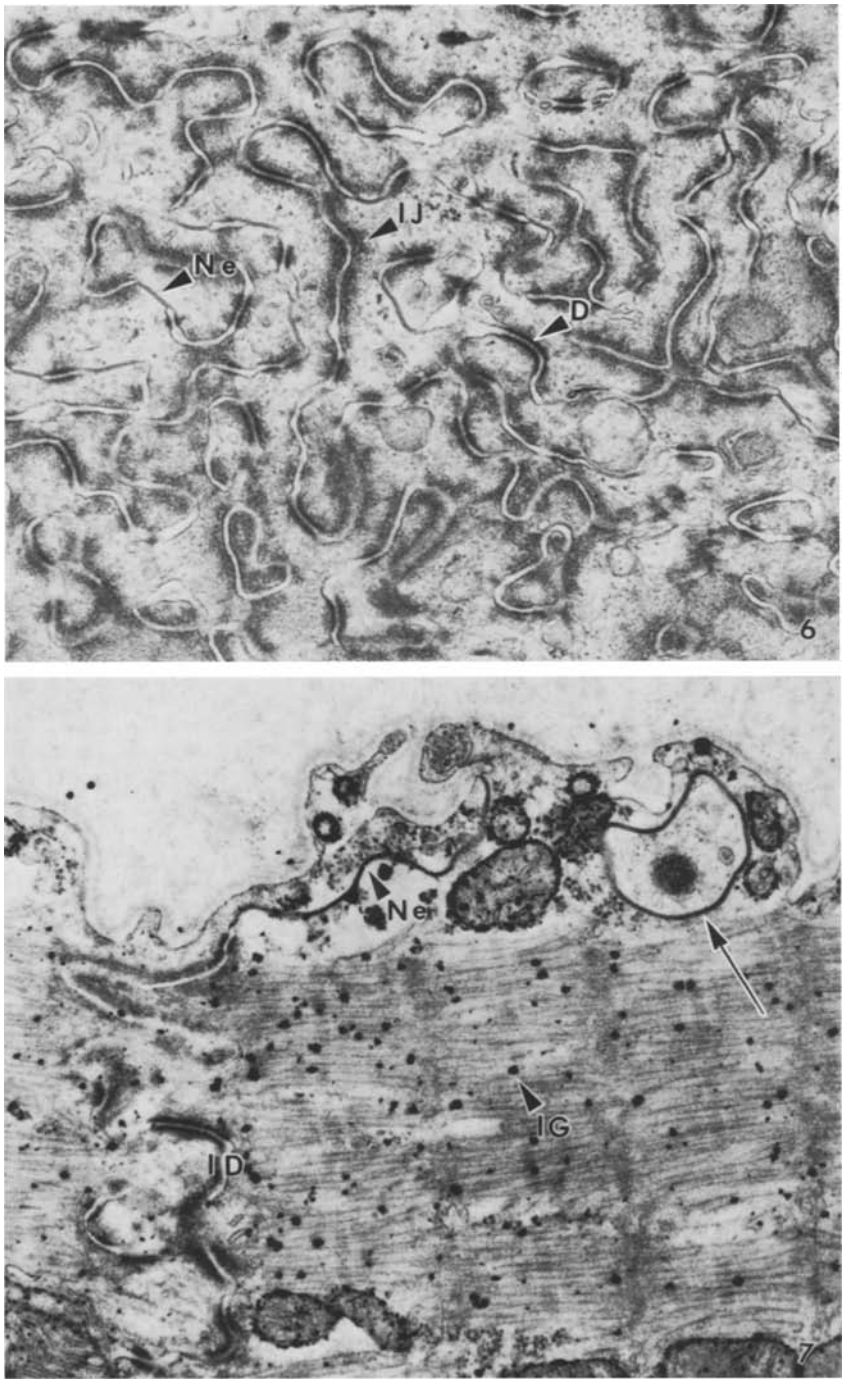

Figs. 6–7. Transverse (**Fig. 6**) and longitudinal (**Fig. 7**) thin sections of the intercalated disc (*ID*) as it is revealed in conventionally stained tissue (**Fig. 6**) and in tissue impregnated with Cu-Pb and poststained with U-Pb (**Fig. 7**). The intercalated disc is composed of an intricate pattern of interdigitated cell membranes, which are joined by a conglomorate of intermediate junctions (*IJ*), desmosomes (*D*) and nexuses (*Ne*). An extensive nexus is situated adjacent to the free cell surface in **Fig. 7** (*Ne*). Note also the circular nexus (*arrow*). *IG*, interfilamentous glycogen particles. Both micrographs, × 25,000

tured preparations where they were located on the P face (Fig. 9).

The T-system was composed of a network of transversely oriented tubular invaginations of the sarcolemma (T-tubules) interconnected by longitudinal (axial) tubules (Figs. 10–16). All membranes of the T-system were similar to the external cell membrane even to the extent of being vested with a laminar coat. The T-tubules, which coursed into the cell interior around the myofibrils and in register with the levels of the Z-band, varied considerably in size, shape and distribution. In some areas they occurred regularly at every Z-band (Figs. 10–11), while in most regions they were few and irregularly distributed (Fig. 5). A three-dimensional display of the T-tubules was achieved by taking stereopair scanning- and transmission electron micrographs of cryofractured material (Fig. 5) and of

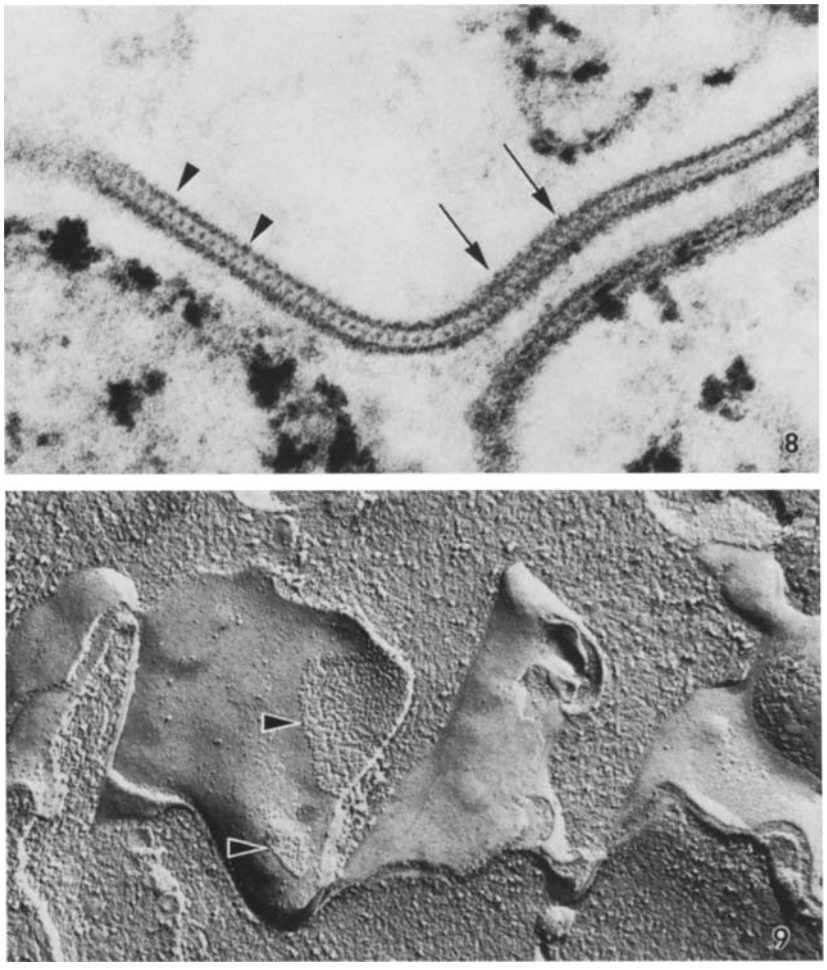

Fig. 8. A detail study of the nexus from Cu-Pb impregnated and U-Pb contrasted tissue. In such material the closely apposed central membranes appear as a dotted line. Punctate opacities are located periodically on the sarcoplasmic sides of the nexus (*arrowheads*). When cut at certain angles the nexus displays a striated pattern (*arrows*). × 200,000

Fig. 9. Freeze fracture replica of the intercalated disc. Arrays of globular subunits of the nexus (connexons) have been exposed on the P face of the split cell membrane (*arrowheads*). × 50,000

thick (1 μm) sections of Cu-Pb impregnated tissue (Fig. 16), respectively. Focal accumulations of Z-band material adjacent to both the sarcolemma and the T-tubular membrane were seen in register with the Z-bands (Figs. 10, 12). The association between the T-tubules and the SR (interior couplings, Figs. 12–16) will be described in conjunction with the latter structure.

Information on the three-dimensional configuration of the SR was obtained by studying thick sections of Cu-Pb-impregnated tissue in the TEM (Figs. 17–21) and cyrofractured material in the SEM (Figs. 4, 22). Most of the intracellular membranous system located in the subsarcolemmal and interfibrillar regions was composed of a continuous branching and anastomosing sarcotubular system. The juxtafibrillar SR revealed a simple but regular pattern, although the degree of sarcotubular branching was not consistent from sarcomere to sarcomere. At the M-band the longitudinal sarcotubules of the A-band region formed a fenestrated collar which only occasionally appeared as a complex network (Fig. 22). At the Z-band level these tubules merged into transversely oriented sarcotubules (Z-tubules), which in the contracted muscle fiber occurred at different levels above the Z-band (Fig. 13). Terminal sarcotubular swellings, corbular SR, were located near the Z-bands (Figs. 4, 22). The sarcotubular system was continuous with the outer nuclear membrane (Fig. 26).

The saccules of the junctional-SR, in association with the sarcolemma proper or with its T-tubular extensions, formed, respectively, peripheral (Fig. 17) and interior (Figs. 12–16) couplings. The flattened saccules were characterized by their electron-dense content and by the periodic densities bridging the narrow gap between the sarcotubules and the plasma membranes (Fig. 12). The peripheral couplings were composed of a single junctional SR saccule oriented in parallel with and in close apposition to the sarcolemma. The interior couplings were organized either as dyads or triads. In the dyad a single SR saccule was positioned to one of either side of the T-tubule, while the

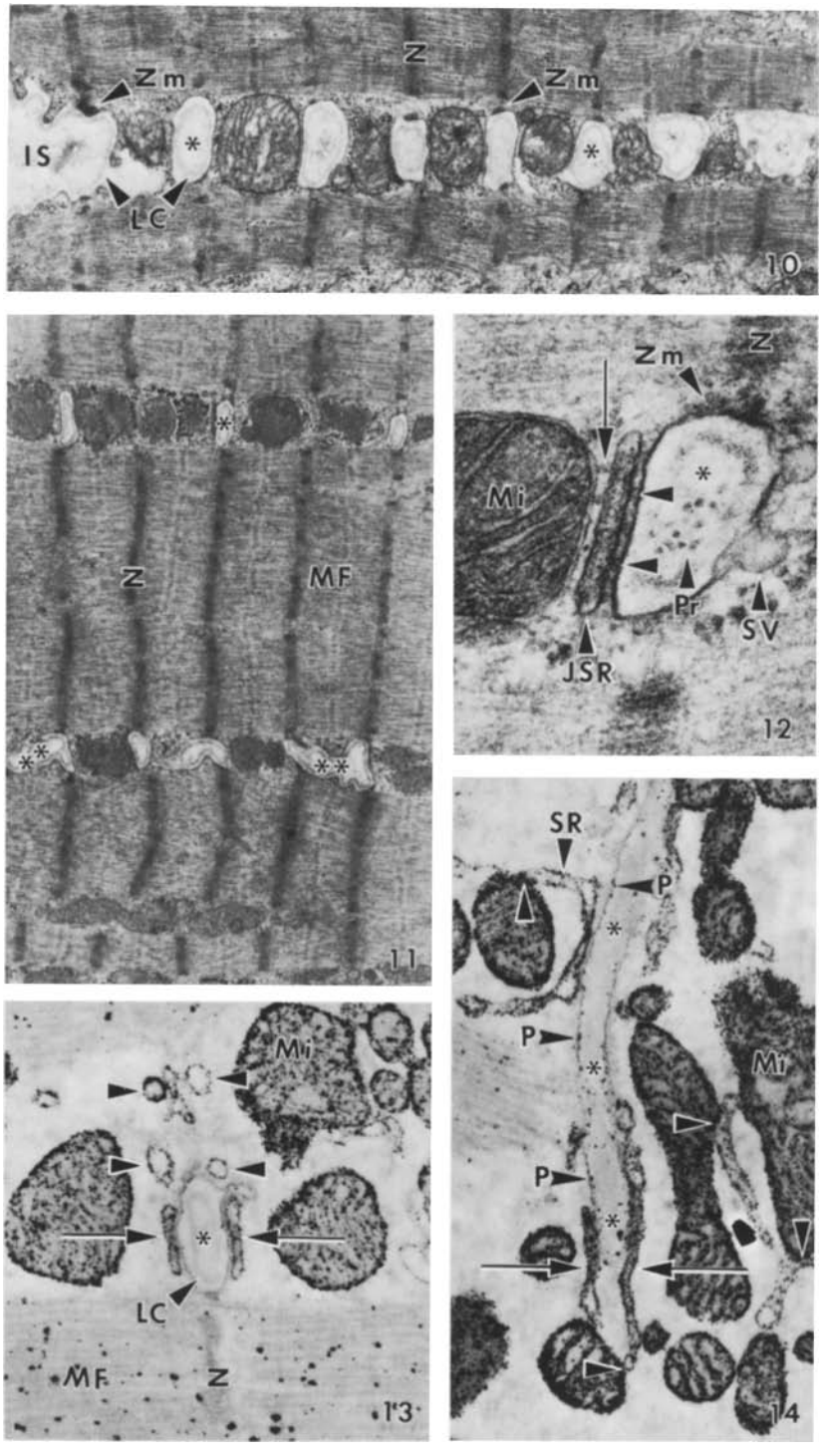

Figs. 10–14. The architecture of the transverse-axial tubular system (T-system) as it is revealed in conventionally stained thin sections (**Figs. 10–12**) and in 1 μm thick sections of Cu-Pb impregnated tissue (**Figs. 13–14**). In the latter case the sarcotubular (*SR*) and mitochondrial (*Mi*) membranes have been selectively stained. The low contrast of the myofibrils (*MF*), the laminar coat (*LC*) and the membranes of the T-system seen in thick sections is due to prolonged exposure to osmium during fixation. Note the presence of a few electron dense particles (*P*) in the T-tubular membrane (**Fig. 14**)
The transverse tubules (single asterisks) open to the intercellular space in register with the Z-bands (*Z*) (**Fig. 10**), and in the cell interior they are interconnected by axial tubules (double asterisks) (**Fig. 11**). The circular profiles (*Pr*, **Fig. 12**) of the tubular lumen may represent cross-sectioned microfibrils. An interior coupling of the dyad type between the transverse tubule and the sarcoplasmic reticulum is depicted in Fig. 12. Junctional processes (*arrowheads*) bridge the narrow gap between the junctional SR (*JSR*) and the tubular membrane. Examples of interior couplings of the triad type are indicated by opposing arrows (**Figs. 13–14**). Transversely running sarcotubules (Z-tubules) indicated by arrowheads, are located superior to the transverse tubule in **Fig. 13**. Note the deposition of Z-band material (*Zm*) at the sarcolemma and at its interior extensions to which the Z-bands are attached (**Figs. 10, 12**). Note also the close apposition between the SR and the mitochondria (*arrowheads*, **Fig. 14**) and the mito-reticular junctional fibers (*arrow*, **Fig. 12**). *SV*, Sarcolemmal vesicle. Fig. 10, ×14,000; Fig. 11, ×10,000; Fig. 12, ×75,000; Figs. 13 and 14, ×30,000

triad was composed of two elements of junctional SR coupled to opposite sides of the T-tubule (Figs. 12–16).

In Cu-Pb impregnated material the various internal cell membranes, including those of the SR, RER, nucleus, mitochondria, Golgi complexes, lysosomes and lipofuscin granules were selectively and densely contrasted (Figs. 2, 13–21, 23–26), whereas, except for a few scattered electron-dense particles, the plasma membranes of the free cell surfaces, the T-tubules and the intercalated discs were not (Figs. 14–17). Glycogen and components of the lipofuscin granules also displayed specific affinity for the stain (Figs. 2, 7, 15, 23–24). Fur-

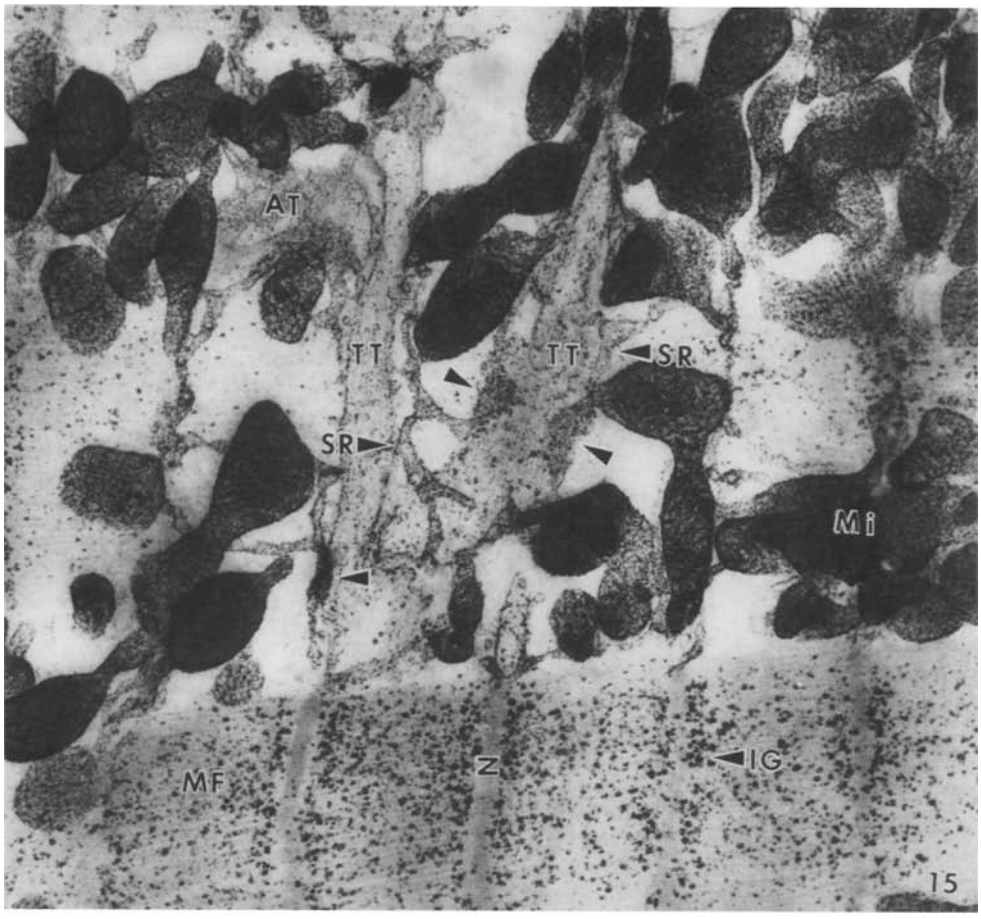

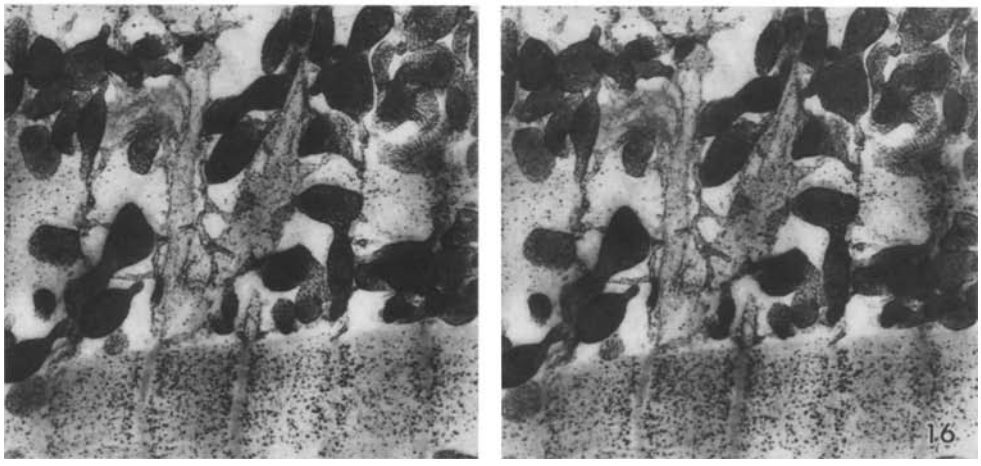

Figs. 15–16. Mono (**Fig. 15**) and stereo-pair (12° tilt) (**Fig. 16**) transmission electron micrographs of a 1 μm thick section of Cu-Pb impregnated tissue demonstrating the three-dimensional relationship between the T-system and the sarcoplasmic reticulum (*SR*). Interior couplings are present both as a dyad (*single arrowhead*) and as a triad (*opposing arrowheads*). Note that the T-tubular membrane contains a few electron-dense particles. *TT*, transverse tubules. *AT*, axial tubule. *MF*, myofibril. *IG*, interfilamentous glycogen particles. *Mi*, mitochondrion. Fig. 15, × 22,000; Fig. 16, × 11,000

thermore, the *en bloc* staining with alkaline Cu-Pb citrate resulted in densely stained particles scattered throughout the heterochromatin portion of the nucleus (Figs. 23, 25–26). In the nucleolus however, the fibrillar component and the fibrillar centres together with the numerous minute particles dispersed throughout the granular component, were selectively contrasted (Figs. 27–28).

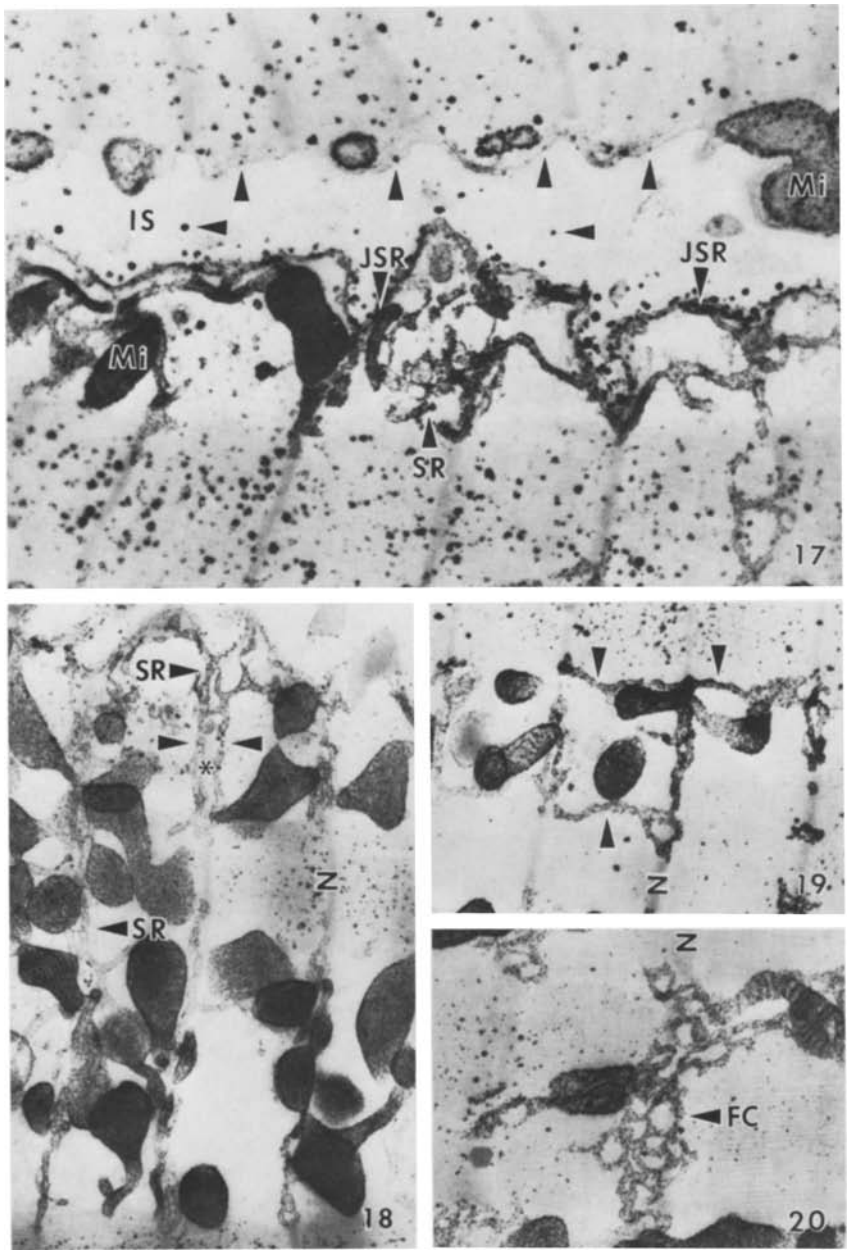

Fig. 17. The sarcotubular network (*SR*) of the surface folds as it appears in a 1 μm thick section of Cu-Pb impregnated tissue. Note that, compared to the densely stained membranes of the SR and the mitochondria (*Mi*), the sarcolemma has no contrast. Like the intercellular space (*IS*) it only contains a few scattered electron-dense particles (*arrowheads*). JSR, junctional SR, ×20,000

Figs. 18–20. Other characteristic patterns of the SR in thick sections (1 μm) of Cu-Pb impregnated tissue. The sarcotubular network of the sarcolemmal folds is continuous with the transverse sarcotubules (Z-tubules) coursing into the cell interior in register with the Z-bands (**Fig. 18**). Some sections reveal that two parallel Z-tubules (*arrowheads*, **Fig. 18**) are located on each side of a T-tubule (*asterisk*). A variable number of longitudinal oriented sarcotubules (*arrowheads*, **Fig. 19**) merges with the Z-tubules at the Z-band (*Z*) level. Sometimes the SR forms a fenestrated collar (*FC*) at the site of the Z-band (Fig. 20). Fig. 18, ×12,500; Fig. 19, ×15,000; Fig. 20, ×17,000

Discussion

This study has shown that by combining different ultrastructural techniques, more extensive knowledge can be obtained of the spatial distribution of various cell components and of their specific staining properties.

The observation by Richter and Kellner (1963) that the myofilaments in the hypertrophied heart maintain their normal size and spatial organization is supported by the present findings. The apparent absence of I-bands is, however, due to fixation of the sarcomeres in the contracted state. According to the observations by Fawcett and McNutt (1969) the I-bands are, at least in cats, the preferential sites of interfilamentous glycogen particles. However, the possibility should be considered that these interfilamentous glycogen particles might be squeezed out from the I-band regions as a consequence of the contraction. They subsequently accumulate adjacent to the Z-bands.

Scanning electron microscopy of the myocardial cell interior has revealed pronounced ridge-like structures traversing the myofibrils at the Z-band level. Several authors have interpreted these structures as T-tubules (McCallister et al. 1974;

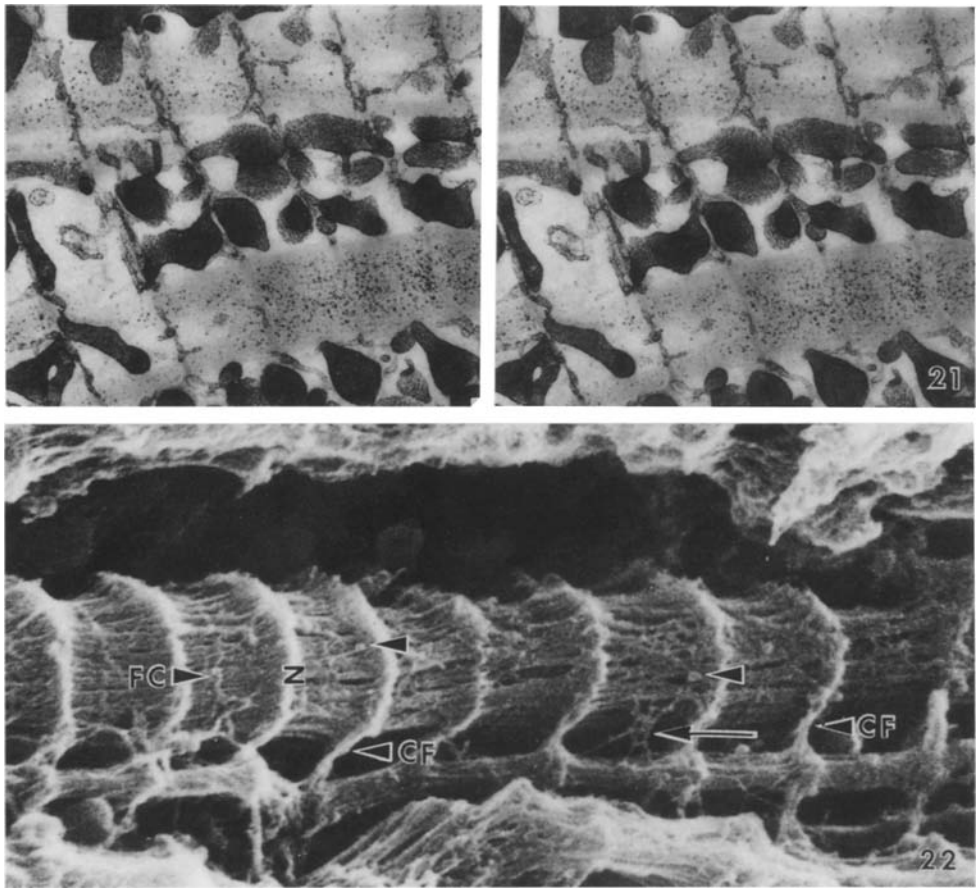

Figs. 21–22. The spatial distribution of the SR as it is revealed in stereopairs (12° tilt) of transmission electron micrographs of 1 μm thick sections of Cu-Pb impregnated tissue (**Fig. 21**) and in a scanning electron micrograph of cryofractured material (**Fig. 22**). Note that both electron microscopic methods have their limitations; TEM due to lack of specimen thickness and SEM due to relatively low resolution. The SEM reveals that the SR forms a fenestrated collar (*FC*) of variable complexity at the M-band level. Note the continuity of the sarcoplasmic reticulum between adjacent myofibrils (*arrow*), and that corbular-SR (arrowheads) occasionally are seen near the elevated Z-bands (*Z*). CF, cytoskeletal filaments, Fig. 21, ×11,000; Fig. 22, ×15,000

Sybers and Ashraf 1974, 1975; Myklebust et al. 1975; Sheldon et al. 1976; Dalen et al. 1978). However, it also has been documented that elevated Z-bands contribute a substantial portion of these ridges (Sybers and Sheldon 1975; Myklebust et al. 1980). This Z-band contribution has been confirmed in the present study by stereoscopic examination of the contracted papillary muscle cell interior.

It remains to be determined whether the extensive nexuses commonly seen in the hypertrophied muscle fiber adjacent to the sarcolemma are a result of abnormal organization during the lateral growth of the muscle fiber, or whether they are morphological manifestations of altered intercellular communication. Since freeze fracture replicas have displayed normal morphology of the globular subunits (connexons) of the nexus, the altered morphology of this junctional complex in the thin sections reported here must be regarded as a fixation artefact. Additional support for this view is found in the observation by Brightman and Reese (1969) that the pentalaminar configuration of the nexus appears or disappears depending on the fixation procedure.

The phylogenetic distribution of the T-system has ben reviewed by Sperelakis et al. (1974). In mammalian hearts the transverse-axial tubules are almost exclusively restricted to the ventricular muscle cells. The sparsely and irregularly distributed T-system of the hypertrophied cardiac muscle shown here is in accordance with the morphology of the non-hypertrophied cristae supraventricularis muscle cell in patients with ventricular septal defect (Maron and Ferrans 1978; Jones and Ferrans 1979). This pattern presents a striking contrast to the well developed and highly organized T-system seen in the right ventricular wall of the mouse heart

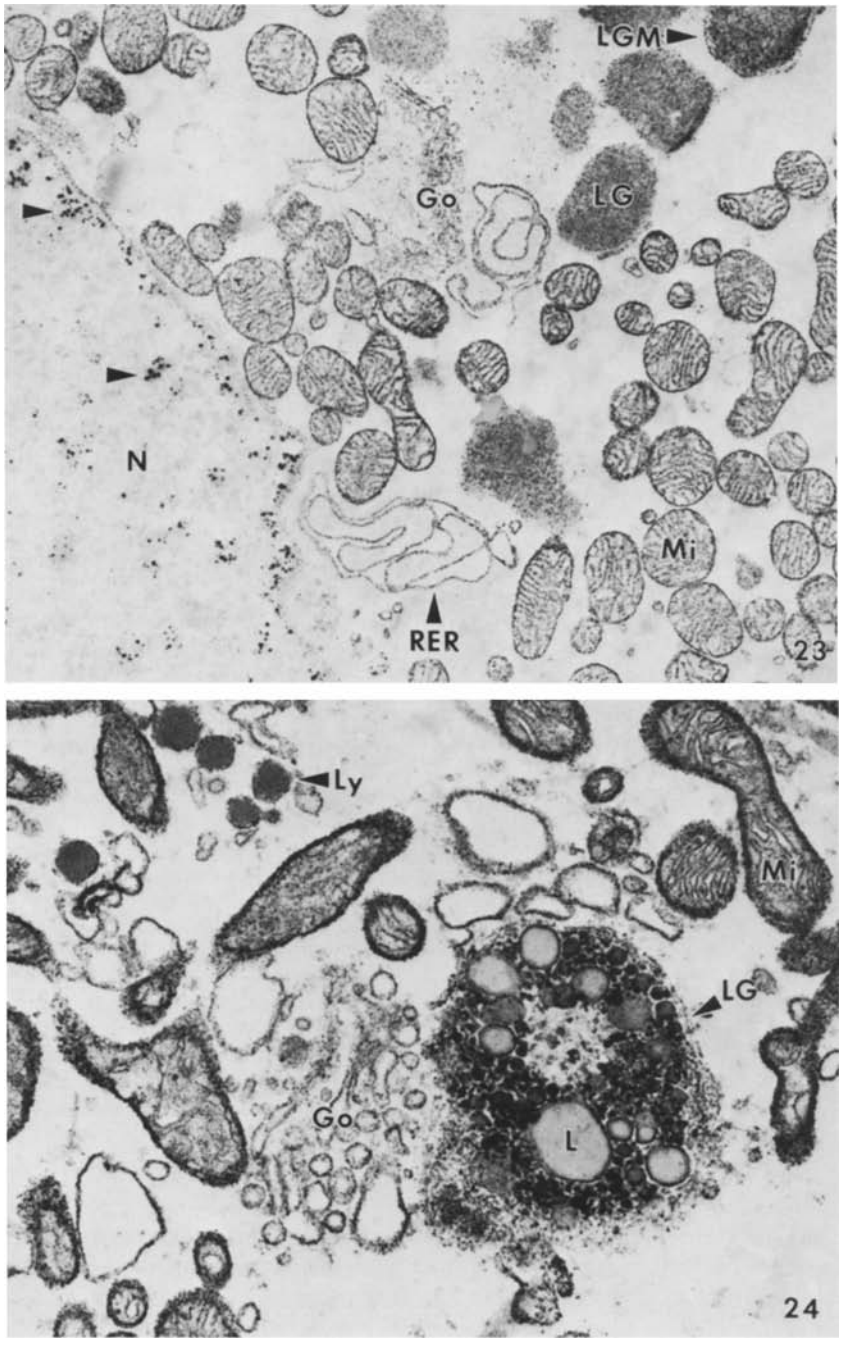

Figs. 23–26. Thin (**Figs. 23–25**) and thick (**Fig. 26**) sections of Cu-Pb impregnated tissue illustrating the selective staining of various cellular elements including the membranes of the nucleus (*N*), mitochondria (*Mi*), Golgi complex (*Go*), rough-surfaced endoplasmic reticulum (*RER*), sarcoplasmic reticulum (*SR*), interfilamentous glycogen particles (*IG*), lysosomes (*Ly*) and their membranes, components of the lipofuscin granules (*LG*) including their membranes (*LGM*), and unidentified particles scatter throughout the heterochromatin (*arrowheads*).

(Forbes and Sperelakis 1983; Forbes et al. 1984). However, it is well documented that the degree of differentiation of the T-system varies in different regions of the heart (Ayettey and Navaratnam 1978) and that the complexity as well as the tubular diameter of this system are species dependent (for review see Forbes and Sperelakis 1983).

The low density of transverse-axial tubules in the present material is in disagreement with previous studies of experimentally induced left ventricular hypertrophy in rats (Page and McCallister 1973; Anversa et al. 1979), which have documented an enhanced proliferation of the membranes of the T-system. However, in a recent study Breisch et al. (1984) have shown that this is the case in the early stage of experimentally induced hypertrophy of the cat ventricle, while the late stage is characterized by reduced surface densities of the T-system.

The literature concerning the ultrastructure

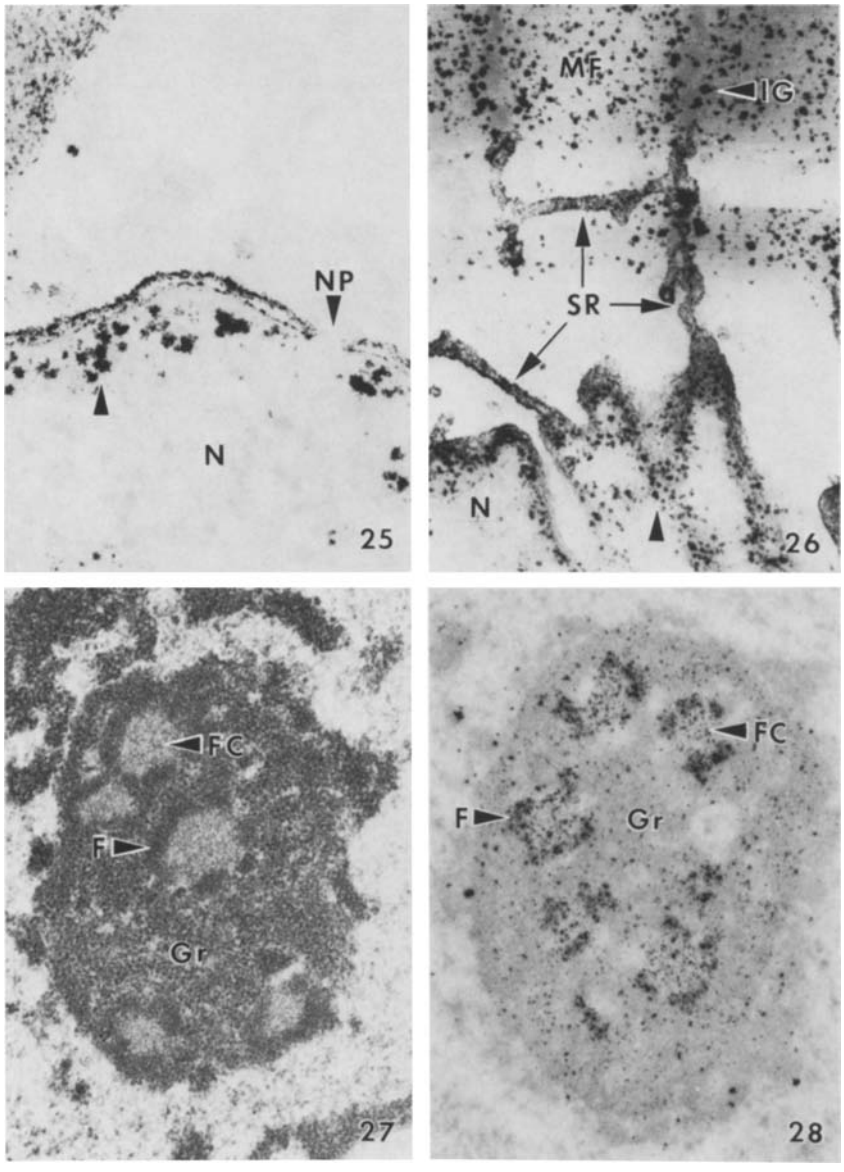

A detail study of the nuclear envelope is shown in **Fig. 25**. The sarcoplasmic reticulum is continuous with the outer nuclear membrane (**Fig. 26**). L, lipid droplet. NP, nuclear pore. MF, myofibril. Fig. 23, ×15,000; Fig. 24, ×30,000; Fig. 25, ×50,000; Fig. 26, ×20,000

Figs. 27–28. The nucleolar ultrastructure differ according to the staining method applied. In conventionally contrasted sections the granular component (*Gr*), the fibrillar component (*F*) and the fibrillar centre (*FC*) are readily identified (**Fig. 27**). After Cu-Pb impregnation the latter two components have been selectively stained, while the granular component appears as a structureless grey background (contrasted by osmium) spotted with intensely stained particles (**Fig. 28**). Both micrographs, ×28,000

and function of the SR has been reviewed by Sperelakis et al. (1974) and by Forbes and Sperelakis (1983). Scanning electron microscopy of cryofractured material combined with transmission electron microscopy of thick sections of tissue specifically stained for the visualization of internal membrane systems offers an improved method for three-dimensional studies of the sarcotubular system. Thus, the application of such techniques in this study and in those of others (Segretain et al. 1981) clearly demonstrates that the transversely oriented Z-tubules are integral parts of the free SR. Filamentous structures anchoring these tubules to adjacent Z-bands (Simpson and Rayns 1968; Edge and Walker 1970; Forbes and Sperelakis 1980) are thought to be instrumental in maintaining the sarcotubular cisternae at proper sarcomere levels during muscle contraction (Segretain et al. 1981). Thus, in the contracted state a multilayered sarcotubular network is found at the Z-band level (Segretain et al. 1981). The sarcotubular elements facing the myofibrils, as presented here, reveal, in general, a strikingly simple pattern compared with the elaborate network seen in other mammals (Sommer and Waugh 1976; Forbes et al. 1977; Van Winkle 1977; Sommer and Johnson 1979; Segretain et al. 1981).

Interconnections between the SR and the outer mitochondrial membrane have previously been reported in gerbil (Dalen et al. 1983) and mouse (Forbes and Sperelakis 1983) ventricular cells. The function of these mito-reticular junctional fibers

remains unknown, although it has been suggested that they may serve as anchoring devices (Dalen et al. 1983).

The physiological role of transverse tubules and SR in exitation – contraction coupling has been well established (Franzini-Armstrong and Peachey 1981; Forbes and Sperelakis 1983). However, architectural differences concerning both the internal (SR-system) and external (T-system) membrane systems undoubtedly result in species-dependent variations of the electrophysical properties and Ca^{2+} metabolism.

Of course, the extent to which the described configuration of the internal and external membrane systems of the hypertrophied muscle fiber differ from those of the normal human heart will remain unknown until such normal tissue becomes accessible for ultrastructural studies. At the same time, differences in the degree of complexity of the sarcotubular system between the papillary muscle and the ventricular wall may also be expected. Support for this view is found in studies on the rat, where the architecture of the juxtafibrillar SR in the papillary muscle (Scales 1983) differs from that in the ventricular muscle (Segretain et al. 1981). However, the possibility of differences in the three-dimensional sarcotubular arrangement caused by different impregnation techniques must be borne in mind.

The observation that the various intracellular membranes stain densely after Cu-Pb impregnation, whereas the plasma membranes of the free cell surfaces, the T-system, and the intercalated discs do not stain, except for the presence of a few scattered electron-dense particles, strongly indicates differences in the chemical and functional properties between the internal and external membrane systems.

At present, the biochemical basis for the results of *en bloc* staining with alkaline Cu-Pb citrate solution is poorly understood (Thiéry and Rambourg 1976). However, in the nucleolus, the selective staining of the fibrillar component and the fibrillar centres is very similar to that obtained in ammoniacal stained (Ag-AS) rat neurons (Pébusque and Seite 1981). This may indicate that the heavy metal ions (Cu^{2+} and/or Pb^{2+}), in the same manner as silver ions, have affinity for the carboxyl groups of acidic non-histone nucleolar proteins, which are known to participate in RNA transcription (Goodpasture and Bloom 1975; Schwarzacher et al. 1978; Olert et al. 1979). If so, the selectively stained particles of the granular component of the nucleolus as well as the peculiar particles present in the heterochromatin region may represent additional sites of specific acidic proteins. Whether or not a similar explanation can be applied to the selective contrast of other cellular components remains an open question. It is, however, tempting to suggest that the granular staining pattern of the various intercellular membranes is a result of specific binding of heavy metal ions (Pb^{2+} and/or Cu^{2+}) to the carboxyl group of the membrane proteins.

Although lead is a well-known capturing agent for the cytochemical localization of phosphatases, consideration of all enzymatic activity in excised material can be excluded following the exposure to low temperature, prolonged fixation in glutaraldehyde and high pH (9–9.5) of the Cu-Pb citrate solution. Nevertheless, the high concentration of Pb^{2+} ions (3,8 mM) in the staining solution used, may have resulted in some cases in ATP hydrolysis (Moses and Rosenthal 1968) and subsequent formation of lead phosphate precipitates.

It seems evident that future ultrastructural studies of hypertrophied myocardial cells will find it appropriate and rewarding to include a variety of ultracytochemical techniques.

Acknowledgement. The biopsy material used in this study was kindly supplied by Dr. Hogne Engedal, Department of Cardiac Surgery, Haukeland Hospital. The constructive criticism of Professor Paul Scheie, Texas Lutheran College, and Professor Melvyn Lieberman, Duke University Medical Center, U.S.A., in the preparation of this manuscript is gratefully acknowledged. We are also indebted to Mr. Jakob Røli, Mrs. Anne Marie Sandsbakk Austarheim and Miss Brynhild Haugen for their technical assistance and to Mrs. Aud Lie-Nilsen for secretarial help.

References

Anversa P, Olivetti G, Melissari M, Loud AV (1979) Morphometric study of myocardial hypertrophy induced by abdominal aortic stenosis. Lab Invest 40:341–349

Ayettey AS, Navaratnam V (1978) The T-tubule system in the specialized and general myocardium of the rat. J Anat 127:125–140

Breisch EA, White FC, Bloor CM (1984) Myocardial characteristics of pressure overload hypertrophy. A structural and functional study. Lab Invest 51:333–342

Brightman MW, Reese TS (1969) Junctions between intimately apposed cell membranes in the vertebrate brain. J Cell Biol 40:648–677

Dalen H (1987) An ultrastructural study of the myocardial cell mitochondria in the hypertrophied human papillary muscle Virchows Arch [Pathol Anat] (submitted)

Dalen H, Myklebust R, Sætersdal TS (1978) Cryofracture of paraffin-embedded heart muscle cells. J Microsc 112:139–151

Dalen H, Scheie P, Myklebust R, Sætersdal T (1983) An ultrastructural study of cryofractured myocardial cells with special attention to the relationship between mitochondria and sarcoplasmic reticulum. J Microsc 131:35–46

Dalen H, Sætersdal TS, Ødegården S (1987) Some ultrastruc-

tural features of the myocardial cells in the hypertrophied human papillary muscle. Virchows Arch [Pathol Anat] (in press)
Echlin P (1975) Sputter coating techniques for scanning electron microscopy. Scan Elect Microsc I:217–224
Edge MB, Walker SM (1970) Evidence for a structural relationship between sarcoplasmic reticulum and Z-lines in dog papillary muscle. Anat Rec 166:51–66
Ericsson JLE, Brunk UT, Arborgh B (1978) Fixation. In: Johannessen JV (ed) Electron Microscopy in Human Medicine, vol 1, McGraw-Hill International Book Company, New York, p 99
Fawcett DW, McNutt NC (1969) The ultrastructure of the cat myocardium. I. Ventricular papillary muscle. J Cell Biol 42:1–45
Ferrans VJ, Butany JW (1983) Ultrastructural pathology of the heart. In: Trump BF, Jones RT (eds) Diagnostic Electron Microscopy, vol. 4. John Wiley and Sons Inc, New York, p 319
Ferrans VJ, Thiedemann K-U (1983) Ultrastructure of the normal heart. In: Silver MD (ed) Cardiovascular Pathology, vol. 1. Churchill Livingstone, New York, p. 31
Forbes MS, Hawkey LA, Sperelakis N (1984) The transverse-axial tubular system (TATS) of mouse myocardium: Its morphology in the developing and adult animal. Am J Anat 170:143–162
Forbes MS, Plantholt BA, Sperelakis N (1977) Cytochemical staining procedures selective for sarcotubular systems of muscle: Modifications and applications. J Ultrastruct Res 60:306–327
Forbes MS, Sperelakis N (1980) Structures located at the levels of the Z bands in mouse ventricular myocardial cells. Tissue & Cell 12:467–489
Forbes MS, Sperelakis N (1983) The membrane systems and cytoskeletal elements of mammalian myocardial cells. In: Dowben RM, Shay JW (eds) Cell and Muscle Mobility, vol. 3. Plenum Press, New York, p 89
Franzini-Armstrong C, Peachey LD (1981) Striated muscle – contractile and control mechanisms. J Cell Biol 91:166s–186s
Goodpasture C, Bloom SE (1975) Visualization of nucleolar organizer regions in mammalian chromosomes using silver staining. Chromosoma 53:37–50
Jones M, Ferrans VJ (1979) Myocardial ultrastructure in children and adults with congenital heart disease. In: Roberts WC (ed) Congenital Heart Disease in Adults. F.A. Davis Company. Philadelphia, p 501
Luft JH (1961) Improvements in epoxy resin embedding methods. J Biophys Biochem Cytol 9:409–414
Maron BJ, Ferrans VJ (1978) Ultrastructural features of hypertrophied human ventricular myocardium. Prog Cardiovasc Dis 21:207–238
McCallister LP, Mumaw VR, Munger BL (1974) Stereo ultrastructure of cardiac membrane systems in the rat heart. Scan Elect Microsc III 713–728
Moses HL, Rosenthal AS (1968) Pitfalls in the use of lead ion for histochemical localization of nucleoside phosphatases. J Histochem Cystochem 16:530–539
Myklebust R, Dalen H, Sætersdal TS (1975) A comparative study in the transmission electron microscope and scanning electron microscope of intracellular structures in sheep heart muscle cells. J Microsc 105:57–65
Myklebust R, Dalen H, Sæterdal TS (1980) A correlative transmission and scanning electron microscopic study of the pigeon myocardial cell. Cell Tissue Res 207:31–41
Olert J, Sawatzki G, Kling H, Gebauer J (1979) Cytological and histochemical studies on the mechanism of the selective silver staining of nucleolus organizer regions (NORs). Histochem 60:91–99
Page E, McCallister LP (1973) Quantitative electron microscopic description of heart muscle cells: Application to normal, hypertrophied and thyroxin-stimulated hearts. Am J Cardiol 31:172–181
Pébusque M-J, Seite R (1981) Electron microscopic studies of silver-stained proteins in nucleolar organizer regions: Location in nucleoli of rat sympathetic neurons during light and dark periods. J Cell Sci 51:85–94
Reynolds ES (1963) The use of lead citrate at high pH as an electron-opaque stain in electron microscopy. J Cell Biol 17:208–212
Richter GW, Kellner A (1963) Hypertrophy of the human heart at the level of fine structure. An analysis and two postulates. J Cell Biol 18:195–206
Robinson TF, Winegrad S (1977) Variation of thin filament length in heart muscle. Nature 267:74–75
Robinson TF, Winegrad S (1979) The measurement and dynamic implications of thin filament lengths in heart muscle. J Physiol 286:607–619
Scales DJ (1983) III. Three-dimensional electron microscopy of mammalian cardiac sarcoplasmic reticulum at 80 kV. J Ultrastruct Res 83:1–9
Schwarzacher HG, Mikelsaar AV, Schnedl W (1978) The nature of Ag-staining of nucleolus organizer regions: Electron- and light-microscopic studies on human cells in interphase, mitosis and meiosis. Cytogenet Cell Genet 20:24–39
Segretain D, Rambourg A, Clermont Y (1981) Three dimensional arrangement of mitochondria and endoplasmic reticulum in the heart muscle fiber of the rat. Anat Rec 200:139–151
Sheldon CA, Friedman WF, Sybers HD (1976) Scanning electron microscopy of fetal and neonatal lamb cardiac cells. J Molec Cell Cardiol 8:853–862
Simpson FO, Rayns DG (1968) The relationship between the transverse tubular system and other tubules at the Z disc levels of myocardial cells in the ferret. Am J Anat 122:193–208
Sommer JR, Johnson EA (1979) Ultrastructure of the cardiac muscle. In: Berne RM, Sperelakis N, Geiger SR (eds) Handbook of Physiology. Section 2: The Cardiovascular System, vol. I: The Heart. The American Physiological Society, Bethesda, p 113
Sommer JR, Waugh RA (1976) The ultrastructure of the mammalian cardiac muscle cell – With special emphasis on the tubular membrane systems. A review. Am J Pathol 82:192–232
Sperelakis N, Forbes MS, Rubio R (1974) The tubular systems of myocardial cells: Ultrastructure and possible function. In: Dhalla NS (ed) Recent Advances in Studies on Cardiac Structure and Metabolism, vol. 4, Myocardial Biology. University Park Press, Baltimore, p 163
Sætersdal TS, Myklebust R, Skagseth E, Engedal H (1976) Ultrastructural studies on the growth of filaments and sarcomeres in mechanically overloaded human hearts. Virch Arch [Cell Pathol] 21:91–112
Sybers HD, Ashraf M (1974) Scanning electron microscopy of cardiac muscle. Lab Invest 30:441–450
Sybers HD, Ashraf M (1975) Scanning electron microscopy of the heart. In: Fleckenstein A, Rona G (eds) Recent Advances in Studies on Cardiac Structure and Metabolism, vol. 6: Pathophysiology and Morphology of Myocardial Cell Alternation. University Park Press, Baltimore, p 305
Sybers HD, Sheldon CA (1975) SEM techniques for cardiac cells in fetal, adult and pathologic heart. (1975). Scan Elect Microsc I:275–280

Thiéry G, Bergeron M (1976) Morphologie spatiale des mitochondries des tubes proximaux et distaux du néphron. Rev Can Biol 35:211–216

Thiéry G, Rambourg A (1976) A new staining technique for studying thick sections in the electron microscope. J Microsc Biol Cell 26:103–106

Trump BF, Smuckler EA, Benditt EP (1961) A method for staining epoxy sections for light microscopy. J Ultrastruct Res 5:343–348

Van Winkle WB (1977) The fenestrated collar of mammalian cardiac sarcoplasmic reticulum: A freeze-fracture study. Am J Anat 149:277–282

Watson ML (1958) Staining of tissue sections for electron microscopy with heavy metals. J Biophys Biochem Cytol 4:475–479

Accepted August 6, 1986